A conserved sequence element in ribonuclease III processing signals is not required for accurate *in vitro* enzymatic cleavage

Bhadrani S.Chelladurai, Honglin Li and Allen W.Nicholson*
Department of Biological Sciences, Wayne State University, Detroit, MI 48202, USA

Received January 29, 1991; Accepted March 14, 1991

ABSTRACT

Ribonuclease III of *Escherichia coli* is prominently involved in the endoribonucleolytic processing of cell and viral-encoded RNAs. Towards the goal of defining the RNA sequence and structural elements that establish specific catalytic cleavage of RNase III processing signals, this report demonstrates that a 60 nucleotide RNA (R1.1 RNA) containing the bacteriophage T7 R1.1 RNase III processing signal, can be generated by *in vitro* enzymatic transcription of a synthetic deoxyoligonucleotide and accurately cleaved *in vitro* by RNase III. Several R1.1 RNA sequence variants were prepared to contain point mutations in the internal loop which, on the basis of a hypothetical 'dsRNA mimicry' structural model of RNase III processing signals, would be predicted to inhibit cleavage by disrupting essential tertiary RNA-RNA interactions. These R1.1 sequence variants are accurately and efficiently cleaved *in vitro* by RNase III, indicating that the dsRNA mimicry structure, if it does exist, is not important for substrate reactivity. Also, we tested the functional importance of the strongly conserved CUU/GAA base-pair sequence by constructing R1.1 sequence variants containing base-pair changes within this element. These R1.1 variants are accurately cleaved at rates comparable to wild-type R1.1 RNA, indicating the nonessentiality of this conserved sequence element in establishing *in vitro* processing reactivity and selectivity.

INTRODUCTION

The maturation of many cellular and viral RNAs in *Escherichia coli* involves specific endonucleolytic cleavages catalyzed by the cell-encoded RNA processing enzyme RNase III [1,2][1]. The presence of RNase III processing signals within primary transcripts can impart metabolic stability [3,4] or instability [5–10] to coding regions upstream or downstream of the processing sites. Moreover, RNase III processing may alter RNA secondary and tertiary structures that block ribosome binding sites, thereby increasing the translational activity of the mRNA [5,11–13]. RNase III has been implicated in regulating gene expression in a manner independent of phosphodiester bond cleavage—a recent study suggests that RNase III binding *per se* to a specific region in bacteriophage lambda cIII mRNA stimulates cIII expression [14], while an earlier study provided evidence that the presence of active RNase III increases the metabolic stability of T4 phage Sp1 RNA [15].

To understand the mechanisms by which gene expression is controlled by RNase III, it is necessary to determine the molecular features in RNase III processing substrates that establish proper enzyme binding and promote specific phosphodiester bond hydrolysis. The nature of the specificity determinant(s) in primary (i.e., those utilized *in vivo* [1,2,16]) RNase III processing signals has remained elusive. Of the approximately thirty viral and cellular primary processing signals that have been currently characterized (either by direct RNA sequence analysis, or indirectly by S1 nuclease mapping, primer extension and/or DNA sequence analysis), all prominently feature RNA-RNA duplex secondary structure. This is not unexpected, as it has been known since the original isolation that RNase III efficiently hydrolyzes double-helical RNA [17]. Several attempts have been made to identify conserved sequence elements in primary processing signals [18–22]; these investigations revealed a conserved CUU/GAA box, or a close variation thereof, which exists in most if not all primary substrates, and is close to the scissile phosphodiester bond(s). The involvement of this sequence in establishing processing signal reactivity or selectivity has not been critically evaluated, although several mutant processing signals which are resistant to cleavage contain base-pair disruptions within this sequence element [7,11].

It has also been argued [23] that tertiary RNA-RNA interactions provide critical identity determinants for many RNase III processing signals. For example, an internal loop (see Figure 1) is a common secondary structural feature of many natural RNase III substrates; however, its involvement in processing reactivity has not been systematically assessed, nor have any mutations which alter or inhibit cleavage been identified which map in this region. Robertson and Barany [24] proposed a hypothetical 'dsRNA mimicry' model for an RNase III processing signal, which served to rationalize the presence of conserved

* To whom correspondence should be addressed

sequence elements within and adjacent to the internal loop of the phage T7 primary processing signals. The conserved T7 sequence elements include the CUU/GAA box, which is located at the base of the upper stem. The structural features of the hypothetical model include coaxial stacking of the upper and lower stems, accompanied by precise folding of the 5′-end and 3′-end-proximal segments of the internal loop into the major grooves of the lower and upper stems, respectively. The proposed folding of the internal loop is stabilized by specific W−C and non-W−C hydrogen bonds, involving base-pair triples. The model displays the overall dimensions of dsRNA, thus exhibiting 'dsRNA mimicry'. The question is whether such a processing signal structure—if it exists—is required for accurate RNase III cleavage.

Our experimental approach towards understanding the structure and function of RNase III processing signals entails the enzymatic synthesis and analysis of small, specific processing substrates, using synthetic DNA oligonucleotides as transcription templates [25,26]. This protocol has been effectively applied to the study of (among others) self-cleaving RNAs [27,28], capsid protein binding sites on viral RNAs [29,30], and the tRNA-synthetase interaction [31,32]. We present herein results which demonstrate that a small (60 nt) RNA, enzymatically generated from a synthetic DNA oligonucleotide encoding the T7 R1.1 processing signal, can be accurately cleaved *in vitro* by RNase III. We show that specific point mutations in the internal loop of the R1.1 processing signal, predicted to disrupt proposed important tertiary RNA-RNA interactions in the dsRNA mimicry model, do not significantly inhibit accurate cleavage by RNase III. We also demonstrate that the CUU/GAA box is not absolutely required for R1.1 processing signal reactivity or cleavage site selection. However, a specific variation of base-pairs adjacent to this element can confer distinct resistance to cleavage, and affect the electrophoretic mobility of the R1.1 RNA in 7M urea-containing polyacrylamide gels.

MATERIALS AND METHODS

Materials

Water used in all experiments was house-distilled, then further purified using a Millipore Milli-Q water system. Chemicals were of the highest grade commercially available. Radiolabeled ribonucleoside triphosphates [α-^{32}P]rUTP (3000 Ci/mmol), [α-^{32}P]rGTP (3000 Ci/mmol), [γ-^{32}P]rATP (6000 Ci/mmol), and [γ-^{32}P]rGTP (6000 Ci/mmol) were obtained from Dupont-NEN (Boston, MA), while unlabeled ribonucleoside triphosphates were from Pharmacia-PL (Piscataway, NJ). Transcription reactions initially used phage T7 RNA polymerase purchased either from New England Biolabs (Beverley, MA) or Promega, Inc. (Madison, WI); subsequent reactions used an in-house preparation of enzyme, isolated from the overexpressing *E. coli* strain BL21 containing plasmid pAR1219 [33]. An initial source of RNase III was provided by H. Robertson; subsequent experiments utilized enzyme obtained from *E. coli* strain HMS174(DE3), which contained the pET-11a [34] plasmid expression vector bearing the *rnc* (RNase III) gene. RNase III was purified according to Chen *et al.* [35], with some modification. Units of RNase III activity were determined as described [17], and the specific activity was 200,000 units/mg for enzyme obtained from HMS174(DE3) cells containing the pET-11a recombinant plasmid. The biochemical properties of RNase III obtained from this system will be described elsewhere (A.W.N. and H.L., in preparation).

Deoxyoligonucleotides were synthesized from β-cyanoethyl-phosphoramidite deoxynucleoside precursors, using either a Beckman System I Plus or an Applied Biosystems Model 380B DNA oligonucleotide synthesizer. Gel-purified [36] deoxyoligonucleotides were stored in water at −20°C, and their molar extinction coefficients were determined as described [37].

Methods

The *in vitro* enzymatic transcription of deoxyoligonucleotides was carried out as described [26]. We did not observe in any of the transcription reactions the production of an 'X' RNA species, as described by Konarska and Sharp [38], either using the commercial or in-house preparations of T7 RNA polymerase. *In vitro* RNase III processing assays were carried out using the reaction buffer and conditions as previously described [39]. Reaction products were analyzed by electrophoresis (23−27 V/cm) in 15% polyacrylamide gels containing TBE buffer and 7M urea. Initial rates of the cleavage reactions were measured by excising gel bands containing the 47 nt product RNA (see Results), and counting in scintillation fluid. Enzymatic RNA sequencing reactions were performed using the enzymes and protocols supplied by the BRL-Life Technologies (Gaithersburg, MD) RNA Sequencing kit. The sequencing reactions and RNase III cleavage products were electrophoresed (36 V/cm) in 10% polyacrylamide gels (0.4mm thick) containing 7M urea in TBE buffer.

RESULTS

DNA Oligonucleotide-directed Enzymatic Synthesis, and Accurate *in vitro* RNase III Cleavage of the T7 R1.1 Primary Processing Signal

The bacteriophage T7 R1.1 primary RNase III processing signal (see Figure 1), which is located between the phage early genes 1 and 1.1 [3,40], provided an appropriate target for enzymatic synthesis from a synthetic deoxyoligonucleotide template. First, it had been previously shown that a recombinant plasmid-encoded 131 nt run-off transcript containing the R1.1 processing signal can be accurately cleaved *in vitro* by RNase III [39]. Second, the R1.1 processing signal secondary structure closely resembles that of the other T7 substrates [3], and in particular the T7 R0.3 primary processing signal, which was used to develop the dsRNA mimicry model [24]. Hence, in addition to allowing a critical evaluation of proposed structures and sequences required for processing reactivity and selectivity, the biochemical analysis of this substrate would have general implications in understanding the structures and reactivities of other RNase III processing signals.

A 77 nt deoxyoligonucleotide was synthesized to encode a strong T7 RNA polymerase class III promoter directly adjacent to a sequence encoding the R1.1 processing signal. Enzymatic transcription *in vitro* would be expected to produce a 60 nucleotide RNA, 55 nucleotides of which comprise the R1.1 processing signal, and the 5 residues at the 5′ end representing promoter-specific nucleotides. Also present in the template is the ϕ1.1A phage polymerase promoter startsite, 8 nucleotides downstream of the R1.1 startsite, and which is a natural component of the R1.1 processing signal [3,40] (see Figure 1). T7 RNA polymerase-catalyzed transcription of the DNA template annealed to its promoter oligonucleotide produced an

approximately 60 nt RNA as the largest species (Figure 2). The synthesis of this RNA was absolutely dependent on DNA template, and in the absence of the promoter oligonucleotide the level of synthesis was only 7% of the complete reaction (data not shown). Transcription of a DNA oligonucleotide encoding a startsite G residue also produced a 60 nt RNA (in about a 5-fold higher yield, compared to the 5′-A-containing transcript; see also [26]), and was also a radiolabeled product using [γ-^{32}P]rGTP (Figure 2). As a check on the correctness of the primary sequence of the RNA (hereafter called R1.1 RNA), 5′-^{32}P-end-labeled transcript was subjected to enzymatic sequencing reactions using the base-specific enzymes RNase T1, RNase U2, and RNase PhyM. Analysis of the products on a sequencing gel (data not shown, but see Figure 3) confirmed the expected proper nucleotide sequence for R1.1 RNA.

The R1.1 RNA is precisely cleaved *in vitro* by RNase III. Thus, treatment of internally radiolabeled R1.1 RNA with RNase III yielded a product of 47 nt, and a doublet species centered at approx. 13−14 nt (Figure 2). Treatment of 5′-^{32}P-end-labeled R1.1 RNA with RNase III produced only the 47 nt fragment as the radiolabeled species (Figure 2), demonstrating that this species carries the 5′end and that the RNase III cleavage site maps at (or very near to) the canonical processing site. Moreover, since the 47 nt fragment is homogeneous, the RNase III cut is precise. The observed heterogeneity of the 3′end-containing fragment is likely a result of the addition of non-templated nucleotides to the 3′end of the transcript during synthesis, which has been discussed elsewhere [25,26]. The presence of intermolecular complexes of substrate (e.g., R1.1 RNA dimers) in the processing reactions was ruled out, since R1.1 RNA which was heated to 90°C, then either snap-cooled on ice, or gradually cooled prior to reaction produced the same RNase III cleavage pattern (data not shown). We have observed occasional variability in the final extents of R1.1 RNA cleavage (e.g., compare Figure 2 with Figure 5) even with excess enzyme; one explanation may be the creation of alternate, stable RNA conformers during synthesis and purification [41,42].

To precisely locate the RNase III cleavage site in R1.1 RNA, the products of RNase III treatment of 5′-^{32}P-labeled R1.1 RNA were electrophoresed in a sequencing gel, along with an alkaline ladder and the products of RNase T1, PhyM and U2 treatment of R1.1 RNA. The results (Figure 3) show that the RNase III-dependent 47 nt RNA has an electrophoretic mobility comparable to a (U-terminated) PhyM reaction product, and migrates approximately one nt faster than a T1 reaction product. The PhyM, U2 and T1 reactions establish the RNase III cleavage site and immediate surrounding sequence to be 5′...UUAU*GAUUG...3′ (the asterisk represents the scissile phosphodiester bond), which is also the *in vivo* cleavage site [43,44]. Thus, R1.1 RNA undergoes faithful processing by RNase III *in vitro*. Closer inspection of the sequencing gel autoradiogram reveals that the RNase III cleavage product migrates slightly more slowly than the PhyM product. This is a result of differing polarities of cleavage: cutting by RNase III creates 5′ phosphomonoester groups [2], while RNase PhyM action creates 3′ phosphomonoester groups [45]. As described elsewhere (e.g., see [46]), the presence of a 3′ terminal

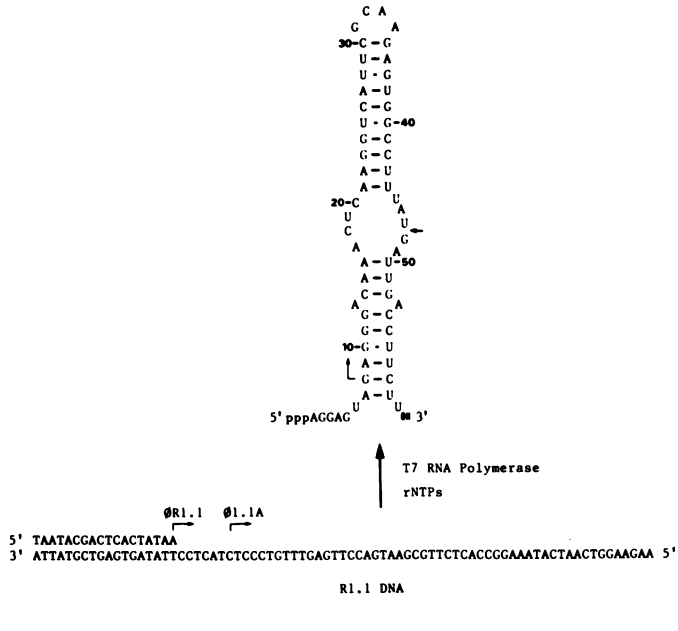

Figure 1. Bacteriophage T7 R1.1 RNase III processing signal: primary and secondary structure, and synthetic deoxyoligonucleotide template. Shown are the 60 nt RNA containing the R1.1 RNase III processing signal, and the corresponding 77 nt transcription template annealed to the 18 nt promoter oligonucleotide. The transcription startsites (+1 nucleotide) for the R1.1 promoter and the ϕ1.1A promoter are indicated by the bent arrows above the DNA template. The DNA template shown here encodes a startsite A nucleotide; a separate template also used in this study encodes a startsite G nucleotide (see text). Shown in R1.1 RNA is the RNase III cleavage site (arrowhead) as well as the startsite nucleotide (G) for the transcript initiated at the ϕ1.1A promoter (bent arrow).

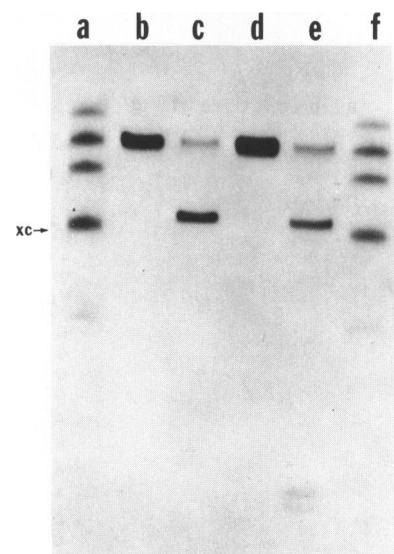

Figure 2. Specific cleavage of R1.1 RNA transcripts by RNase III. R1.1 RNA was synthesized either in the presence of [α-^{32}P]rUTP or [γ-^{32}P]rGTP, and purified as described in Materials and Methods. Portions (1065 dpm) of internally- or end-labeled R1.1 RNA were treated with RNase III (0.15 units) in 20 μl volumes at 37°C for 30 minutes, then electrophoresed in a 7M urea-containing 15% polyacrylamide gel. Lanes (b) and (c) display 5′ end-labeled R1.1 RNA incubated in the absence [lane (b)] or presence [lane (c)] of RNase III. Lanes (d) and (e) display internally-labeled R1.1 RNA incubated in the absence [lane (d)] or presence [lane (e)] of RNase III. Lanes (a) and (f) display RNA size markers, generated by *in vitro* transcription by T7 RNA polymerase of pBSII SK(+) plasmid (Stratagene, Inc., La Jolla, CA) cut either by SmaI, EcoRI, EcoRV, ClaI, XhoI, or ApaI restriction endonucleases (the ApaI-cleaved DNA was treated with T4 DNA polymerase prior to transcription). From top to bottom, the RNA lengths are: 73, 63, 55, 44 and 30 nt (the 17 nt ApaI-specific transcript was not included in these gel lanes). The position of migration of the xylene cyanol (xc) dye is indicated on the left hand side of the figure.

phosphomonoester group increases the gel electrophoretic mobility of an RNA oligonucleotide; however, the relative mobility shift is attenuated as the RNA chain length increases, due to a decreasing change in the charge-to-mass ratio. The alkaline ladder of 5'-end-labeled R1.1 RNA revealed a distinct region of strong band compression, occurring from approximately nucleotides 41 to 43 (Figure 3). The band compression indicates the stability of the upper stem double helix, and in particular suggests the importance of the two adjacent G-C base pairs near the base of the upper stem (see Figure 1) in establishing the upper stem duplex structure.

Biochemical Reactivity of R1.1 RNA Internal Loop Sequence Variants

Several sequence variants of R1.1 RNA were prepared to contain specific point mutations in the internal loop region. These alterations were expected to disrupt tertiary RNA-RNA interactions proposed to occur in a dsRNA mimicry model of the R1.1 RNA internal loop [24] (see Introduction). The prediction would be that the mutant R1.1 RNAs, lacking the internal loop dsRNA mimicry structure, would be strongly resistant to cleavage by RNase III. Specifically, R1.1 mutant N1 contains a U to A change at position 45, expected to disrupt a proposed base triple, involving nucleotide residue C20 interacting with the A17-U45 W−C bp (Figure 4; see [24] for the precise molecular structures). R1.1 mutant N10 displays an A to U change at position 17, which is expected to disrupt the same C20-A17-U45 base triple. Mutant N2 contains two alterations (A to U at position 17, and U to A at position 45) which would reestablish a W−C bp across the internal loop—formally absent with R1.1 mutants N1 and N10—and perhaps restore or even increase cleavage reactivity. R1.1 mutants N3, N24 and N25 exhibit a change from G48 to A, C or U, respectively; these substitutions would abolish two (non W−C) hydrogen bonds in a proposed G23-C42-G48 base triple, thereby disrupting folding of the 3' segment in the major groove of the upper stem. R1.1 mutants N4, N4a and N5 exhibit C to U changes at position 42, or 41, or both 42 and 41, respectively, creating wobble G-U bp. N4 and N5 would exhibit a weakened G23-C42-G48 base triple interaction, as well as reducing the duplex stability of the R1.1 upper stem.

As a check on the correctness of the synthesized mutant RNA sequences, 5'-^{32}P-end-labeled N3 RNA was sequence-analyzed, and shown to specifically lack an RNase T1 cleavage site mapping at position 48 (data not shown), but which is present in wild-type (N0) R1.1 RNA (see Figure 3). Internally-radiolabeled mutant RNAs were compared with N0 RNA for their reactivity towards RNase III, as assayed in a time course experiment[2]. To assess the relative initial cleavage rates, the amounts of the 47 nt RNA product were directly measured from excised gel bands. The results, shown in Figure 5, indicate that all the R1.1 RNA sequence variants are cleaved by RNase III. The mutant RNA cleavage products comigrate with the N0 RNA products, indicating that the canonical scissile bond is recognized in all cases. The N1 and N10 RNAs are processed at rates comparable to N0 RNA. The N2, N3 and N5 RNAs are cleaved somewhat more slowly than N0 RNA (Figure 5A,B). Thus, N3 RNA was cleaved 3.8-fold more slowly than N0 RNA; by inference, the N2 and N5 RNAs exhibit comparably-reduced cleavage rates. N24 and N25 RNAs are cleaved at rates essentially the same as N0 RNA (data not shown). Since these R1.1 sequence variants can be processed at similar rates and with the same specificity as wild-type R1.1 RNA, we conclude that the proposed dsRNA mimicry structure is not strictly required for processing reactivity. However, the reduced reactivities of N2 and N3 RNAs suggest that base alterations within the internal loop region can, albeit

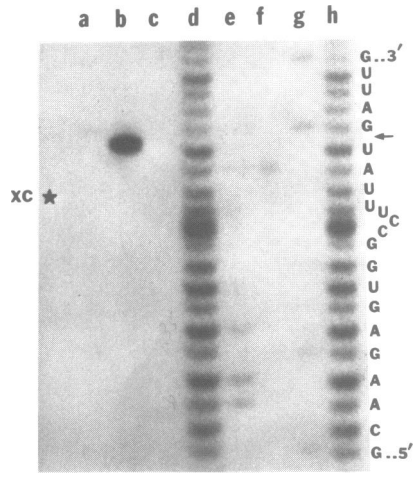

Figure 3. Mapping the RNase III cleavage site in R1.1 RNA. 5' end-labeled R1.1 RNA (500 dpm) was treated with RNase III (0.1 unit) in a 10 μl reaction volume for 40 minutes at 37°C. A parallel reaction omitted RNase III. Aliquots (75 dpm) of the RNA products were electrophoresed in a 15% polyacrylamide thin sequencing gel. Parallel lanes included an aliquot (3000 dpm) of R1.1 RNA incubated (90°, 15 min) in 0.5 M $NaHCO_3/Na_2CO_3$ (pH 9.2) (alkaline ladder) or a portion (1800 dpm) treated with RNase PhyM, or a portion (940 dpm) treated with RNase T1, or a portion (930 dpm) incubated with RNase U2. Lane (a), RNase T1 reaction; lane (b), R1.1 RNA treated with RNase III; lane (c), R1.1 RNA incubated in the absence of RNase III; lane (d), alkaline ladder; lane (e), PhyM reaction; lane (f), RNase U2 reaction; lane (g), RNase T1 reaction; lane (h), alkaline ladder. The xylene cyanol (xc) blue dye marker is indicated on the left side. The sequence at the right side shows the primary RNA sequence surrounding the R1.1 cleavage site; the band compression (see Results) is indicated by the local deviation of the sequence from a straight vertical line. The arrow marks the RNase III cleavage site.

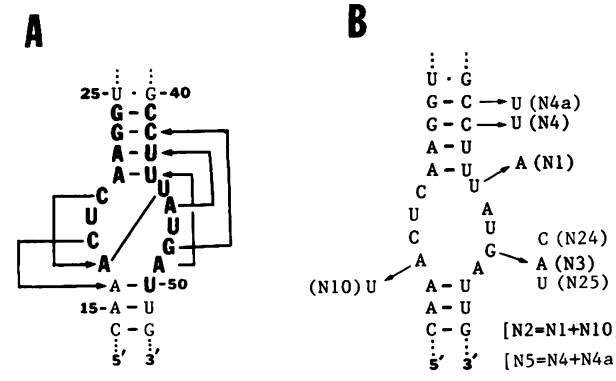

Figure 4. The dsRNA mimicry model, and R1.1 RNA sequence variants containing point mutations within the internal loop of the R1.1 processing signal. Panel A schematically indicates the proposed tertiary RNA-RNA interactions within the T7 R1.1 primary RNase III processing signal. The bold-faced nucleotide residues indicate the region of conserved sequence seen in the T7 processing signals [24]. The diagonal line within the internal loop indicates a proposed W−C bp between residues A17 and U45. The jointed arrows indicate proposed base triples, formed between internal loop bases, and bp in the upper or lower stems. Panel B displays the sites of base changes in the mutant R1.1 processing signals. The names of the mutant R1.1 RNAs are given within the parentheses. N2 and N5 are double mutants.

to a modest extent, influence cleavage reactivity. The decreased reactivity of N5 RNA probably reflects a requirement for stable upper stem duplex structure; N5 RNA is similar in structure and reactivity to a previously-described cleavage-resistant T7 R0.3 processing signal mutant [13]. Closer examination of the N0 RNA time course in Figure 5B reveals the modest production of approximately 30 nt and 20 nt RNA species, appearing at the 10 and 40 minute time points. These products probably result from additional cleavage of the 47 nt RNA product, occurring 5′ to residue C20. Cleavage at this site would release a 19 nt 5′end-containing fragment, and a 28 nt fragment containing the upper stem. This low efficiency reaction is not seen in any of the R1.1 sequence variants, and may be the result of RNase III recognizing a secondary cleavage site which is situated opposite the primary site, and formally offset by two nucleotides. A similar reactivity pattern has been observed with the T7 R1.3 processing signal [11].

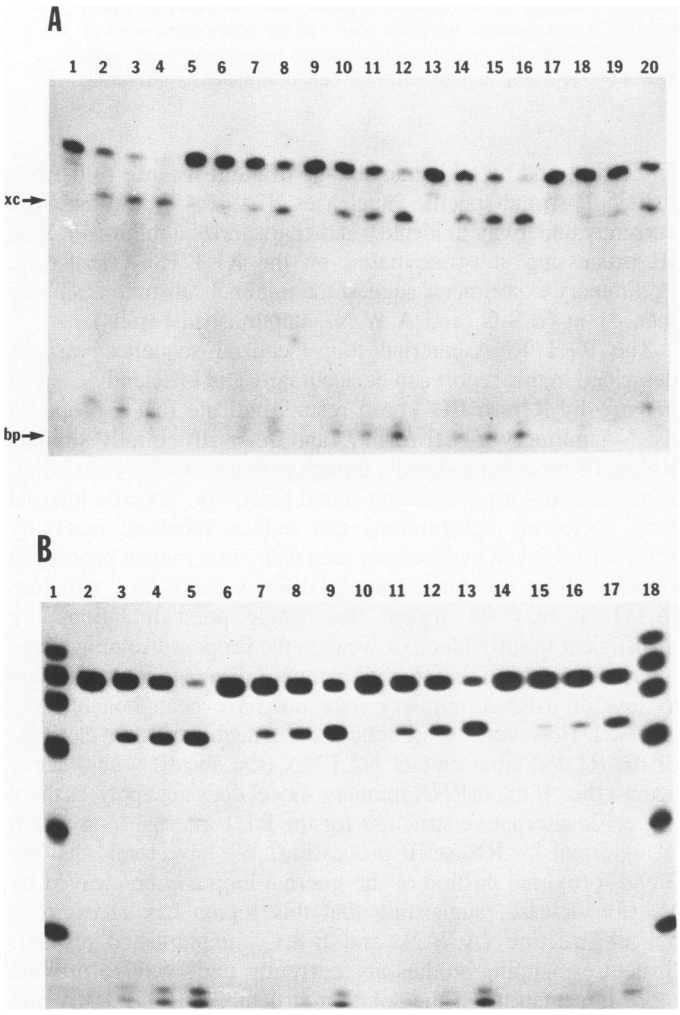

Figure 5. Testing the dsRNA mimicry model for the R1.1 processing signal. Wild-type (N0) R1.1 RNA, and mutants N1, N2, N3, N4, N4a, N5 and N10 were synthesized in radiolabeled form using [α-^{32}P]rUTP, and purified as described in Materials and Methods. The RNAs (2500 dpm, 0.18 pmol) were incubated at 30°C with RNase III (0.2 units) in 25 μl volumes. Aliquots (5 μl) were removed at 5, 10 and 40 minutes and electrophoresed in 7M urea-containing 15% polyacrylamide gels. (A): Lanes (1−4) show N0 RNA reaction products following incubation for 40 minutes in the absence of RNase III [lane (1)], or following incubation for 5 [lane (2)], 10 [lane (3)] or 40 [lane (4)] minutes with RNase III. Lanes (5−8) represent the corresponding time course for mutant N3 RNA; lanes (9−12) represent the time course for mutant N1 RNA; lanes (13−16) represent the time course for mutant N10 RNA; and lanes (17−20) represent the time course for mutant N2 RNA. The positions of migration of the xylene cyanol (xc) and bromphenol blue (bp) dyes are indicated on the left hand side of the figure. (B): Lanes (2−5) display the N0 RNA time course (0,5,10,40 minutes, respectively); lanes (6−9) display the corresponding N4 RNA time course; lanes (10−13) display the corresponding N4a RNA time course, and lanes (14−17) the N5 RNA time course. Lanes (1) and (18): RNA size markers (see legend to Figure 2).

A Conserved RNA Sequence Element is not Essential for R1.1 Processing Reactivity or Specificity

On the basis of its conserved nature and proximity to the scissile phosphodiester bond(s), a CUU/GAA base-paired sequence (nts 21−23, and 42−44 in R1.1 RNA; see Figures 1 and 4) has been proposed to be in some manner important in directing RNase III processing [18−22]. In support of this, several previous studies which characterized cleavage-resistant RNase III substrates revealed mutations which changed this sequence, and also disrupted the W−C base-pairing that is strictly conserved within this element [6,7,11]. However, it was not determined whether cleavage resistance was conferred by destabilization *per se* of the double-helical structure, or by altering the CUU/GAA sequence.

We assessed the role of the CUU/GAA element in establishing the *in vitro* reactivity of RNase III processing signals by analyzing R1.1 RNA sequence variants which contained specific base-pair substitutions within the upper stem-localized 4 bp (CCUU/GGAA) segment (Table 1). This element is present in most of the T7 processing signals, and includes the CUU/GAA box. The mutant RNAs maintained a full complement of base-pairs, and the upper stem thermodynamic stabilities were comparable to that of wild-type R1.1 RNA (Table 1). The RNAs were synthesized in internally radiolabeled form, and their reactivity to RNase III tested in a time course assay. The results of a representative assay are displayed in Figure 6, where it is seen that the R1.1 variants N8(UCCU/AGGA), N27(UCGU/AGCA), N35(UGGU/ACCA) and N36(UGCU/ACGA) RNAs are cleaved at rates comparable to that of N0(CCUU/GGAA) RNA. Also, N20(CAAC/GUUG) and N30(CCGU/GGCA) RNAs exhibited reactivities essentially the same as that of N0 RNA (data not shown). The canonical scissile bond is utilized in all of the sequence variants, since the 3′ end-containing cleavage products comigrate with the 3′ end-containing fragment of the N0 RNA reaction products (Figure 6). We conclude that the CUU/GAA sequence box is not essential for *in vitro* processing reactivity or selectivity. Figure 6 also shows that the N0 RNA time course produced a small amount of an approximately 30 nt RNA fragment, probably resulting from a minor amount of secondary cleavage reaction (see above).

A Cleavage-Resistant Upper Stem-Localized Sequence Variant of R1.1 RNA which exhibits an Altered Gel Electrophoretic Mobility

In screening R1.1 upper stem sequence variants, we found one species which exhibited a distinct resistance to enzymatic cleavage. Specifically, N11 RNA is similar to N35 RNA, except for the replacement of the UG and CG base-pairs, directly above the CUU/GAA sequence box, by two GC bp (see Table 1). N11 RNA exhibits a significantly-reduced cleavage rate compared to N35 RNA in a time course assay (Figure 6B). The relative cleavage rate reduction of N11 relative to N35 RNA was

Table 1. Biochemical Reactivities of R1.1 RNA Sequence Variants Containing Base-Pair Alterations in the CUU/GAA Conserved Sequence Element.

	CG	CG	CG	CG	CG	CG	CG	CG	CG	CG	GC
	UG	UG	UG	UG	UG	UG	UG	UG	UG	UG	GC
	GC-41	UA	CG	GC	CG	GC	AU	AU	AU	AU	AU
Sequence[a]:	GC	UA	CG	UA	AU	GC	GC	GC	CG	CG	CG
	AU	CG	UA	UA	AU	CG	GC	CG	GC	CG	CG
	21-AU	CG	UA	GC	CG	AU	AU	AU	AU	AU	AU
Name:	N0	N12	N15	N20	N21	N30	N8	N27	N36	N35	N11
Reactivity[b]:	(+++)	+++	+++	+++	+++	+++	+++	+++	+++	+++	++

(a): refer to Figure 1 for position of the conserved sequence element within the R1.1 processing signal; the numbers with N0 (wild-type) RNA refer to position within the R1.1 primary sequence. The bold-face letters in NO RNA indicate the CUU/GAA sequence box; the bold-face letters in N12-N11 RNAs indicate the changes from the N0 sequence. The calculated [57] thermodynamic stabilities ($\Delta H°$) of the upper stems were of comparable magnitude, and ranged between −46(N12) and −56(N30) kcal/mol. (b): Reactivities were measured using a time-course assay, with limiting substrate and at 160 mM KCl.[2] The '++' for N11 RNA is equivalent to a two-fold drop in initial cleavage rate, determined by measuring amounts of product RNA in initial rate experiments (see Results).

determined to be 2-fold (N35 RNA has a comparable reactivity to N0 RNA). The reduced reactivity is not obviously due to base-pair disruption or otherwise reduced upper stem stability (see Table 1). Thus, it appears that specific base-pair substitution next to the CUU/GAA sequence box can influence processing reactivity. This region exhibits no sequence conservation among primary processing signals, and the inhibition could be due to changes in RNA structure, with concomitant alteration of nucleotide-protein contacts.

The base-pair alterations also affect the physical behavior of N11 RNA. When N11 and N0 RNAs are denatured with glyoxal and electrophoresed on a 10 mM phosphate buffer-containing polyacrylamide gel, they comigrate at the 60 nt position (data not shown). However, Figures 6B and 7A reveal that N11 RNA displays a distinctly retarded gel electrophoretic mobility on polyacrylamide gels containing 7M urea: N11 RNA electrophoreses more slowly than the 63 nt RNA size marker, while N0 RNA migrates ahead of the same size marker at the expected (60 nt) position (Figure 7A). Partial cleavage of N11 RNA by RNase III produces a large RNA product which comigrates with the 44 nt RNA size marker, while the large N0 RNA produce migrates at the same position (Figure 7A) (note that the N0 and N11 13/14 nt RNA doublet products comigrate, indicating utilization of the same cleavage site). When urea is omitted from the 15% polyacrylamide gel (Figure 7B), the electrophoretic mobility of N11 increases, relative to N0 RNA and the RNA size markers. In this system, N0 and N11 RNAs migrate substantially faster than the 63 nt RNA size marker, probably due to the presence of the compact upper stem hairpin structure. We conclude that in the presence of 7M urea, N11 RNA, and its large RNase III cleavage product assume conformations that are distinctly different from those of N0 and N35 RNA.

DISCUSSION

This report has demonstrated that a small RNA containing the phage T7 R1.1 processing signal can be accurately cleaved *in vitro* by RNase III. Hence—and as anticipated by an earlier study [39]—the RNA determinants required for accurate RNase III processing are contained within an approximately 60 nt irregular RNA hairpin structure. Other small RNase III processing signals previously characterized were dsRNA species, containing complementary RNA segments flanking the 23S rRNA and 16S rRNA sequences in the 30S rRNA precursor [24,48,49]. These substrates could be accurately processed *in vitro*, and were able to be isolated due to the accumulation of 30S RNA in RNase III-strains, and by taking advantage of the resistance of dsRNA to single-strand-specific nucleases [24,48,49]. Studies are currently underway to identify and characterize a minimal RNase III processing substrate based on the R1.1 RNA structure. Preliminary experiments suggest the minimal substrate is smaller than 41 nt (B.S.C. and A.W.N., unpublished results).

The R1.1 RNA internal loop-localized sequence variants described in this report can be accurately and efficiently cleaved *in vitro* by RNase III. These results indicate that a proposed dsRNA mimicry model for T7 (and other structurally similar) RNase III processing signals, though perhaps capable of existing, is not essential for processing signal reactivity. Specific internal loop nucleotide substitutions can reduce substrate reactivity somewhat, but not to the extent seen with other mutant processing signals which exhibit disrupted dsRNA secondary structure [6,11]. It may be argued that single point mutations are insufficient to fully block or weaken the proposed folding of the internal loop, such that the full extent of cleavage inhibition due to loss of dsRNA mimicry may not have been conclusively assessed. However, the accurate and reasonably efficient cleavage of the R1.1 double mutant N2 RNA (see above) would argue against this. If the dsRNA mimicry model does not apply, is there a specific alternative structure for the R1.1 internal loop which is important for RNase III processing? We have found that the 3'end- proximal portion of the internal loop can be cleaved by V_1 ribonuclease, suggesting that this region has access to a helical structure (A.W.N. and B.S.C., unpublished results). Structure mapping studies are currently underway to provide more information on the solution structure of R1.1 RNA and specific sequence variants. A recent study has analyzed the influence of bulge loops on RNA structure [50]; perhaps the internal loop may provide a specific overall shape that is important for reactivity of R1.1 RNA, as well as other RNase III processing signals.

This study has also shown the dispensable nature *in vitro* of the CUU/GAA sequence box, a strongly-conserved feature of primary RNase III processing signals. All of the R1.1 RNA CUU/GAA sequence box variants examined in this study were accurately and efficiently cleaved, showing that the conserved sequence is not involved in cleavage specificity, nor does it apparently strongly influence cleavage efficiency. None of the mutant processing signals exhibited more rapid cleavage kinetics than the wild-type substrate; perhaps the CUU/GAA sequence box represents an RNA element that confers optimal processing efficiency. However, several cautionary notes are required in assessing the role of the CUU/GAA box (or any other sequence or structure) in establishing processing signal reactivity. First,

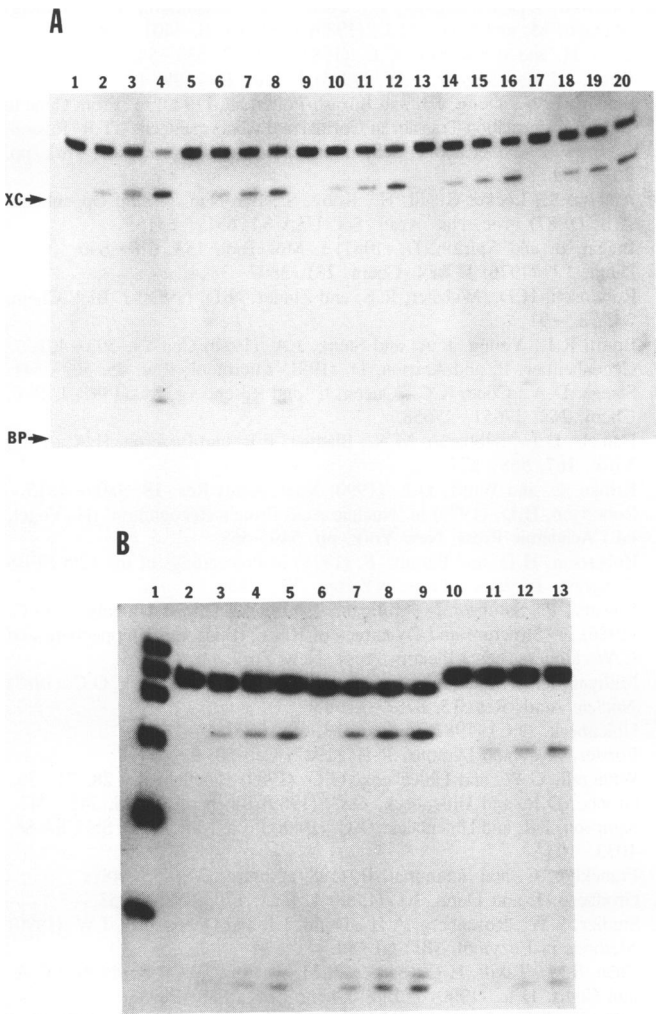

Figure 6. Testing the involvement of the CUU/GAA sequence box in establishing R1.1 RNA processing reactivity. R1.1 RNAs N0, N8, N11, N27, N35 and N36 (see Table 1) were synthesized in internally-radiolabeled form and purified as described in Materials and Methods. (A): Time course assays were performed on N0, N8, N27, N35 and N36 RNAs (2500 dpm, 0.09 pmol) at 30°C in 25 μl reactions containing 0.16 units of RNase III. Aliquots (5 μl) were taken at 0, 5, 10 and 40 minutes and analyzed by gel electrophoresis. Lanes (1–4); N0 RNA (0,5,10,40 minutes, respectively); lanes (5–8): N8 RNA; lanes (9–12): N27 RNA; lanes (13–16): N35 RNA; lanes (17–20): N36 RNA. 'XC' and 'BP' mark the position of the xylene cyanol and bromphenol blue electrophoresis dyes. (B): Time course assays were performed on N0, N11 and N35 RNAs. Experimental conditions were as described above, except that 0.4 units of RNase III were used. Aliquots (2000 dpm; 0.07 pmol) were removed at 0, 5, 10 and 40 minutes and analyzed. Lanes (2–5): N35 RNA; lanes (6–9): N0 RNA. Lanes (10–13): N11 RNA. Lane (1) displays RNA size markers (see legend to Figure 2).

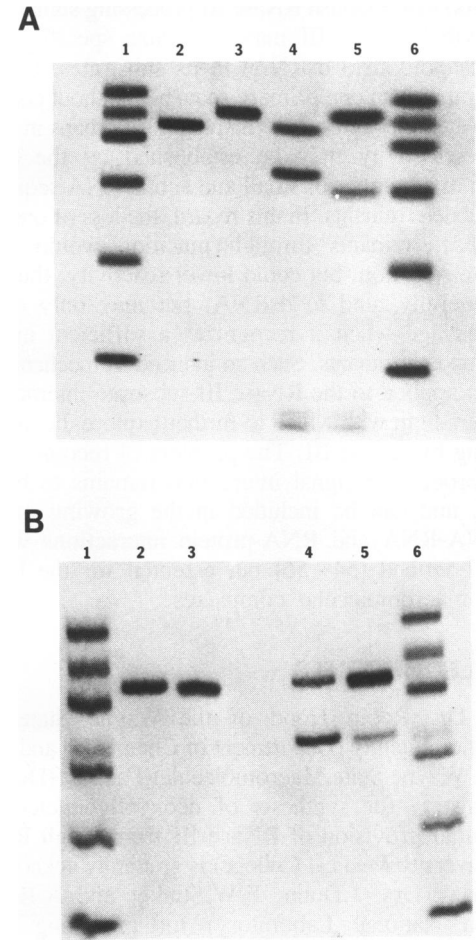

Figure 7. Altered gel electrophoretic mobility of an R1.1 RNA upper stem sequence variant. N35 and N11 RNAs were synthesized in radiolabeled form and purified as described in Materials and Methods, then subjected to gel electrophoretic analysis either with or without prior reaction with RNase III (0.24 units). (A): Analysis of N35 and N11 RNAs and their RNase III cleavage products on a 15% polyacrylamide gel containing 7M urea. Lane (2), N35 RNA (600 dpm); lane (3), N11 RNA (600 dpm); lane (4), N35 RNA (1,250 dpm) partially reacted with RNase III; lane (5), N11 RNA (1,250 dpm) partially reacted with RNase III. Lanes (1) and (6): RNA size markers. (B): N35 and N11 RNAs electrophoresed on a 15% polyacrylamide gel without urea. The order of the lanes is the same as in (A). The small RNase III cleavage products were also produced, but migrated ahead of the 17 nt RNA size marker, and are not shown in this panel.

to the extent that RNase III processing signals may also have other biological roles (such as in transcription [5]), conserved sequences or structures may be important for these other functions. Second, *in vitro* processing reactivities may not be directly extrapolatable to the situation *in vivo*. The levels of RNase III in the cell are low [35], and competition between processing signals may be significant in establishing the *in vivo* processing efficiency of any given substrate. Third, RNase III activity *in vivo* may be modulated by other cellular factors [35,51]. In investigating the report of an ATP-binding site on RNase III [35], we have found no effect of added ATP on the rate of R1.1 RNA cleavage *in vitro* (A.W.N. and B.S.C., unpublished results). Experiments are underway to correlate *in vivo* and *in vitro* reactivity patterns of specific R.1 sequence variants. Moreover, a steady-state kinetic analysis of RNase III-catalyzed cleavage of R1.1 RNA will provide detailed information on the binding (K_m) and catalytic (k_{cat}) steps of this reaction.

Other than the CUU/GAA sequence box, there are no other obvious sequence similarities shared by primary RNase III processing signals [21,22]. We have recently found that all but three bp of the R1.1 upper stem may be removed, or alternatively the upper stem can be lengthened, without altering cleavage site selection (A.W.N. and B.S.C., unpublished results). Thus, the available evidence does not support the model that RNAse III is a 'molecular ruler', which measures in from one end of a dsRNA segment to select the cleavage site [1,22]. Given the results of this study and others, what may be the true specificity

determinant(s) that establish RNase III processing signal reactivity and selectivity? RNase III may recognize specific structural features (in addition to dsRNA) in its substrates, that can be attained by more than one primary sequence without concomitant loss of cleavage selectivity. Alternatively (or perhaps in addition), processing selectivity may be established by the collective cooperation of a number of small and subtle RNA sequence and structural subdeterminants. In this regard, the loss of one, or even several subdeterminants through mutation would not alter cleavage site selection, but could lower reactivity; thus, RNase III may generally bind to dsRNA, but may only efficiently catalyze cleavage when it recognizes a sufficient number of specificity subdeterminants. Such an induced-fit mechanism (e.g., see [52,53]) applied to the RNase III-substrate interaction may provide a paradigm with which to further explore the mechanism of processing by RNase III. The problem of recognition in the RNase III-processing signal interaction remains to be clearly understood, and can be included in the growing number of specific RNA-RNA and RNA-protein interactions which are currently ill-defined [54–56] but essential for the biological function of macromolecular complexes.

ACKNOWLEDGEMENTS

We thank Dr. Robin Hood of the Wayne State Central Instrumentation Facility (Department of Chemistry) and Dr. June Snow of the Wayne State Macromolecular Facility (Department of Biochemistry) for synthesis of deoxyoligonucleotides. A generous initial provision of RNase III from Hugh Robertson (Cornell University Medical College) is gratefully acknowledged. We also thank Drs. J.Dunn, F.W.Studier and A.Rosenberg (Brookhaven National Laboratory) for providing plasmids pAR1219 and pAR2637. The efforts of J.Butler in assembling the manuscript, and comments by Dr. A.Siegel are much appreciated. This work was supported by Grant GM-41283 to A.W.N. from the National Institutes of Health, and by the Center for Molecular Biology, Wayne State University.

[1] Abbreviations used: RNase III, Ribonuclease III [E.C.3.1.24]; TBE buffer, 89 mM Tris base, 89 mM Boric acid, 10 mM EDTA; nt, nucleotide; bp, base pair; ds, double-stranded; W–C, Watson-Crick.

[2] The KCl concentration was maintained at 160 mM in all of the *in vitro* processing assays, in order to assess primary cleavage site reactivity under near-physiological conditions [16]. In the time course assays, the initial cleavage reaction velocity was proportional to the amount of enzyme added; moreover, the substrate concentration was kept low, in order that the relative initial rates would be a function of the specificity constant (k_{cat}/K_m) [47].

REFERENCES

1. Robertson, H.D. (1982) Cell **30**, 669–672.
2. Dunn, J.J. (1982) in 'The Enzymes' vol. 15, (P. Boyer, ed.) Academic Press, New York, pp 485–499.
3. Dunn, J.J. and Studier, F.W. (1983) J. Mol. Biol. **166**, 477–535.
4. Panayotatos, N. and Truong, K. (1985) Nucleic Acids Res. **13**, 2227–2240.
5. Gottesman, M., Oppenheim, A. and Court, D. (1982) Cell **29**, 727–728.
6. Guarneros, G., Montanez, C., Hernandez, T. and Court, D. (1982) Proc. Nat. Acad. Sci. USA **79**, 238–242.
7. Schmeissner, U., McKenney, K., Rosenberg, M. and Court, D. (1984) J. Mol. Biol. **176**, 39–53.
8. Portier, C., Dondon, L., Grunberg-Manago, M. and Regnier, P. (1987) EMBO J. **6**, 2165–2170.
9. Regnier, P. and Grunberg-Manago, M. (1989) J. Mol. Biol. **210**, 293–302.
10. Bardwell, J.C.A., Regnier, P., Chen, S.M., Nakamura, Y., Grunberg-Manago, M. and Court, D.L. (1989) EMBO J. **8**, 3401–3407.
11. Saito, H. and Richardson, C.C. (1981) Cell **27**, 533–542.
12. Dunn, J.J. and Studier, F.W. (1975) J. Mol. Biol. **99**, 487–499.
13. Studier, F.W., Dunn, J.J. and Buzash-Pollert, E. (1979) in 'From Gene to Protein: Information Transfer in Normal and Abnormal Cells' (T.R. Russell, K. Brew, H. Faber and T. Schultz, eds.) Academic Press, New York, pp. 261–269.
14. Altuvia, S., Locker-Giladi, H., Koby, S., Ben-Nun, O. and Oppenheim, A.B. (1987) Proc. Nat. Acad. Sci. USA **84**, 6511–6515.
15. Pragai, B. and Apirion, D. (1981) J. Mol. Biol. **153**, 619–630.
16. Dunn, J.J. (1976) J. Biol. Chem. **251**, 3807–3814.
17. Robertson, H.D., Webster, R.E. and Zinder, N.D. (1968) J. Biol. Chem. **243**, 82–91.
18. Bram, R.J., Young, R.A. and Steitz, J.A. (1980) Cell **19**, 393–401.
19. Gegenheimer, P. and Apirion, D. (1981) Microbiol. Rev. **45**, 502–541.
20. Steege, D.A., Cone, K.C., Queen, C. and Rosenberg, M. (1987) J. Biol. Chem. **262**, 17651–17658.
21. Daniels, D.L., Subbarao, M.N., Blattner, F.R. and Lozeron, H.A. (1988) Virol. **167**, 568–577.
22. Krinke, L. and Wulff, D.L. (1990) Nucl. Acids Res. **18**, 4809–4815.
23. Robertson, H.D. (1977) in 'Nucleic Acid-Protein Recognition' (H. Vogel, ed.) Academic Press, New York, pp. 549–568.
24. Robertson, H.D. and Barany, F. (1978) in Proceedings of the 12th FEBS Congress, Pergamon Press, NY, pp. 285–295.
25. Lowary, P., Sampson,J., Milligan, J., Groebe, D. and Uhlenbeck, O.C. (1986) in 'Structure and Dynamics of RNA' (P.H. van Knippenberg and C.W. Hilbers, eds.) Plenum Press, New York, pp. 69–76.
26. Milligan, J.F., Groebe, D.F., Witherell, G.W. and Uhlenbeck, O.C. (1987) Nucleic Acids Res. **15**, 8783–8798.
27. Uhlenbeck, O.C. (1987) Nature 328, 596–600.
28. Forster, A.C. and Symons, R.H. (1987) Cell **50**, 9–16.
29. Witherell, G.W. and Uhlenbeck, O.C. (1989) Biochemistry **28**, 71–76.
30. Groebe, D.R. and Uhlenbeck, O.C. (1989) Biochemistry **28**, 742–747.
31. Sampson, J.R. and Uhlenbeck, O.C. (1988) Proc. Natl. Acad. Sci USA **85**, 1033–1037.
32. Francklyn, C. and Schimmel, P. (1989) Nature **337**, 478–481.
33. Grodberg, J. and Dunn, J.J. (1988) J. Bact. **170**, 1245–1253.
34. Studier, F.W., Rosenberg, A.H., Dunn, J.J. and Dubendorff, J.W. (1990) Methods in Enzymol. **185**, 60–89.
35. Chen, S.M., Takiff, H.E., Barber, A.M., Dubois, W.C., Bardwell, J.C.A. and Court, D.L. (1990) J. Biol. Chem. **265**, 2888–2895.
36. Atkinson, T. and Smith, M. (1984) in 'Oligonucleotide Synthesis: A Practical Approach' (M.J. Gait, ed.) IRL Press, Oxford pp. 35–81.
37. Sproat, B.S. and Gait, M.J. (1984) *ibid*, pp. 83–115.
38. Konarska, M.M. and Sharp, P.A. (1989) Cell **57**, 423–431.
39. Nicholson, A.W., Niebling, K.R., McOsker, P.L. and Robertson, H.D. (1988) Nucleic Acids Res. **16**, 1577–1591.
40. Oakley, J.L. and Coleman, J.E. (1977) Proc. Nat. Acad. Sci. USA **74**, 4266–4270.
41. Heus, H.A., Uhlenbeck, O.C., and Pardi, A. (1990) Nucleic Acids Res. **18**, 1103–1108.
42. Walstrum, S.A. and Uhlenbeck, O.C. (1990) Biochemistry **29**, 10573–10576.
43. Rosenberg, M., Kramer, R.A. and Steitz, J.A. (1974) Brookhaven Symp. Biol. **26**, 277–285.
44. Robertson, H.D., Dickson, E. and Dunn, J.J. (1977) Proc. Nat. Acad. Sci. USA **74**, 822–826.
45. Donis-Keller, H. (1980) Nucleic Acids Res. **8**, 3133–3142.
46. Auron, P.E., Weber, L.D. and Rich, A. (1982) Biochemistry **21**, 4700–4706.
47. Fersht, A. (1985) 'Enzyme Structure and Mechanism' (2nd Edition), W.H. Freeman and Co., NY.
48. Robertson, H.D., Pelle, E.G. and McClain, W.H. (1980) in 'tRNA: Biological Aspects'. Cold Spring Harbor Laboratory Press, Cold Spring Harbor, NY, pp. 107–122.
49. Gegenheimer, P. and Apirion, D. (1980) Nucleic Acids Res. **8**, 1873–1891.
50. Tang, R.S. and Draper, D.E. (1990) Biochemistry **29**, 5232–5237.
51. March, P.E. and Gonzalez, M.A. (1990) Nucleic Acids Res. **18**, 3293–3298.
52. Lesser, D.R., Kurpiewski, M.R. and Jen-Jacobsen, L. (1990) Science **250**, 776–786.
53. Heitman, J. and Model, P. (1990) EMBO J. **9**, 3369–3378.
54. Jones, M.H. and Guthrie, C. (1990) EMBO J. **9**, 2555–2561.
55. Draper, D.E. (1989) Trends Biochem. Sci. **14**, 335–338.
56. Altman, S. (1990) J. Biol. Chem. **265**, 20053–20056.
57. Freier, S.M., Kierzek, R., Jaeger, J.A., Sugimoto, N., Caruthers, M.H., Neilson, T. and Turner, D.H. (1986) Proc. Nat. Acad. Sci. USA **83**, 9373–9377.